HHS Public Access

Author manuscript

Development. Author manuscript; available in PMC 2017 July 12.

Published in final edited form as:

Development. 2007 November ; 134(21): 3837–3848. doi:10.1242/dev.011361.

Cortical granule exocytosis in *C. elegans* is regulated by cell cycle components including separase

Joshua N. Bembenek[1,*], **Christopher T. Richie**[2], **Jayne M. Squirrell**[1], **Jay M. Campbell**[1], **Kevin W. Eliceiri**[1], **Dmitry Poteryaev**[3], **Anne Spang**[3], **Andy Golden**[2], and **John G. White**[1]

[1]University of Wisconsin-Madison, Laboratory of Molecular Biology, 1525 Linden Drive, Madison, WI 53706, USA [2]Laboratory of Biochemistry and Genetics, NIDDK, National Institutes of Health, Building 8, Room 323, 8 Center Drive, Bethesda, MD 20892-0840, USA [3]Growth and Development, Biozentrum, University of Basel, Klingelbergstrasse 50/70, CH-4056 Basel, Switzerland

Abstract

In many organisms, cortical granules undergo exocytosis following fertilization, releasing cargo proteins that modify the extracellular covering of the zygote. We identified cortical granules in *Caenorhabditis elegans* and have found that degranulation occurs in a wave that initiates in the vicinity of the meiotic spindle during anaphase I. Previous studies identified genes that confer an embryonic osmotic sensitivity phenotype, thought to result from abnormal eggshell formation. Many of these genes are components of the cell cycle machinery. When we suppressed expression of several of these genes by RNAi, we observed that cortical granule trafficking was disrupted and the eggshell did not form properly. We conclude that osmotic sensitivity phenotypes occur because of defects in trafficking of cortical granules and the subsequent formation of an impermeable eggshell. We identified separase as a key cell cycle component that is required for degranulation. Separase localized to cortically located filamentous structures in prometaphase I upon oocyte maturation. After fertilization, separase disappeared from these structures and appeared on cortical granules by anaphase I. RNAi of *sep-1* inhibited degranulation in addition to causing extensive chromosomal segregation failures. Although the temperature-sensitive *sep-1(e2406)* allele exhibited similar inhibition of degranulation, it had minimal effects on chromosome segregation. These observations lead us to speculate that SEP-1 has two separable yet coordinated functions: to regulate cortical granule exocytosis and to mediate chromosome separation.

Keywords

Anaphase promoting complex; Cortical granule exocytosis; Egg activation; Separase; Spindle assembly checkpoint; *C. elegans*; Meiosis

[*]Author for correspondence (jbembenek@wisc.edu).

Supplementary material

Supplementary material for this article is available at http://dev.biologists.org/cgi/content/full/134/21/3837/DC1

INTRODUCTION

Oocytes must coordinate specialized meiotic divisions with fertilization and the subsequent transition to the mitotic program. Egg activation comprises a sequence of events that occur in response to calcium transients triggered by fertilization, including cortical granule exocytosis and resumption of the cell cycle. Cortical granules are large vesicles located at the cortex of mature oocytes of many species. Cortical granules secrete a collection of proteoglycans and enzymes that modify the extra embryonic covering of oocytes to prevent polyspermy (Wessel et al., 2001). At fertilization, inactivation of cytostatic factor, which arrests oocytes in metaphase through inhibition of an E3 ubiquitin ligase known as the anaphase-promoting complex/cyclosome (APC/C), allows entry into anaphase and resumption of the cell cycle (Tunquist and Maller, 2003).

In the *Caenorhabditis elegans* gonad, oocytes arrested in prophase I undergo maturation in response to signals from sperm and are subsequently ovulated (Yamamoto et al., 2006). After fertilization in the spermatheca, embryos pass into the uterus and extrude two polar bodies during consecutive meiotic divisions. Eggshell formation in nematodes occurs during meiosis (Chitwood and Chitwood, 1974), such that the first polar body remains outside the permeability barrier, whereas the second polar body does not (Polinko and Strome, 2000). The *C. elegans* eggshell consists of three layers, which we describe according to the following nomenclature: the outermost vitelline layer present around the mature oocyte; a middle chitinous layer necessary for mechanical strength; and an internal lipid layer providing the permeability barrier (Rappleye et al., 1999; Wharton, 1980). Although the process of eggshell formation in *C. elegans* is poorly understood, a recent genome-wide screen identified 109 genes likely to be required for eggshell formation (Sonnichsen et al., 2005), some of which are cell cycle regulatory components, suggesting a link between cell cycle regulation and eggshell formation.

Regulation of cell division requires faithful orchestration of a wide diversity of cellular processes. During M-phase, precise regulatory mechanisms ensure the fidelity of chromosome segregation and cell cleavage. During metaphase, a complex signaling pathway known as the spindle-assembly checkpoint (SAC) prevents entry into anaphase before the correct alignment of chromosomes on the metaphase plate (Musacchio and Salmon, 2007). The SAC preserves chromosome cohesion by inhibiting the APC/C (Peters, 2006). At the metaphase to anaphase transition, APC/C ubiquitinates securin, an inhibitory chaperone of the protease separase, leading to its degradation by the proteasome (Nasmyth, 2002). Active separase then cleaves a subunit of the cohesin complex, allowing the poleward movement of chromosomes during anaphase.

Inactivation of the *C. elegans* ortholog of separase, *sep-1*, causes chromosome nondisjunction, the osmotic integrity defective phenotype (OID) and cytokinesis failures (Siomos et al., 2001). The osmotic integrity defective phenotype is also caused by inhibition of a number of cell cycle regulatory components (Sonnichsen et al., 2005), and has been suggested to be a non-specific consequence of meiotic division failures. However, loss of other cell cycle genes that cause severe meiotic defects does not give rise to an OID

phenotype (Polinko and Strome, 2000), indicating that eggshell deposition is separable from cell division, although these processes may be linked.

We have found that cortical granules form in developing oocytes and are exocytosed, leading to the formation of an impermeable three-layered eggshell in *C. elegans*. The exocytosis of cortical granules occurs during anaphase I and requires a number of cell cycle components, including separase. During anaphase I, separase localizes to cortical granules and may have a direct role in regulating cortical granule exocytosis. Our observations indicate that events occurring during egg activation are coordinated by cell cycle regulatory controls in *C. elegans*.

MATERIALS AND METHODS

C. elegans strains and alleles

The wild type was the Bristol strain N2, and all strains were cultured using standard techniques (Brenner, 1974). Temperature-sensitive strains were maintained at 16°C and shifted to 25°C as L4 animals; all other strains were maintained at 20°C. The following strains were also used: WH0216 {*sep-1(e2406)* I /hT2[*bli-4(e937) let-?(q782) qIs48*]}, WH0213 {*sep-1(e2406)* I; *unc-119(ed3)* III, *ruIs32* III*[GFP::His-58 unc119(+)]*/ hT2[*bli-4(e937) let-?(q782) qIs48*]}, HY604 *mat-1(ye121)* I, AZ212 {*unc-119(ed3)* III, *ruIs32* III*[GFP::His-58 unc119(+)]*}, WH0327 {*unc-119(ed3)* III, *ojIs23[GFP::SP12 unc119(+)]*}, WH0351 {*unc-119(ed3)* III, *ojIs37[GFP::UGTP-1 unc119(+)]*}, RT688 {*unc-119(ed3)* III, *pwIs281[GFP::CAV-1 unc119(+)]*}, WH0416 {*unc-119(ed3)* III, *ojIs58[SEP-1::GFP unc119(+)]*}, WH0438 {*unc-119(ed3)* III, *ojEx64[GFP::SEP-1 unc119(+)]*}.

Molecular biology

cDNA clones for *syn-4* (yk493b10.3), *cpg-1* (also known as *cej-1* – WormBase) (yk253a11) and *cpg-2* (yk1687e03) were subcloned into the L4440 vector for feeding RNAi (Kamath et al., 2001). Separase feeding RNAi was performed as previously described (Siomos et al., 2001), and all other constructs were obtained from the Ahringer library (Kamath et al., 2003). L4 animals were fed at 20°C for 24 hours (Fig. 4C–F), or as otherwise noted. The 2.5 kb *ugtp-1* (ZK370.7) coding region was cloned from genomic DNA into the pID3.01 vector for biolistic transformation, as described in (Poteryaev et al., 2005). The 5.2 kb coding sequence of *sep-1* was amplified from N2 genomic DNA using Phusion polymerase (NEB, Ipswich, MA, USA) and subcloned into the pJK derivative plasmids of pFJ1.1 (Verbrugghe and White, 2004) that allow for directional cloning, and *pie-1*-driven expression of N- and C-terminal fusions with several worm-optimized fluorescent proteins including mGFP (A206K mutant). Biolistic transformation was done as previously described (Praitis et al., 2001).

Immunohistochemistry and staining

The last 438 amino acids of the *sep-1* open reading frame fused to a hexahistidine tag expressed in bacteria was purified using the Probond protein purification kit as per the manufacturer's protocol (Invitrogen, Carlsbad, CA, USA) under denaturing conditions in 8

M urea. This purified protein was concentrated, dialyzed and used to raise rabbit polyclonal antibodies following standard protocols (Covance Research Products, Berkeley, CA, USA). The resulting immune serum was affinity-purified against antigen that had been gel-purified and immobilized on nitrocellulose paper. Embryo staining was performed as described in Gonczy et al. (Gonczy et al., 1999) to preserve membrane structures. The following dilutions, in PBS+0.05% BSA, were used: α-SEP-1 antibodies, 1:200; α-HIM-10 antibodies, 1:50; rhodamine-lectins from Vector Laboratories, 1:10; tubulin antibody DM1α (Sigma, St Louis, MO, USA), 1:100; Alexa-conjugated secondary antibodies (Invitrogen), 1:200; and TO-PRO-3 Iodide (Invitrogen), 1:500. FM2–10 (Invitrogen) was used at 17 μM, FM4–64 was used at 0.02 mg/ml and a fluorescein-conjugated 3000-MW dextran (Invitrogen) was used at 0.5 mg/ml in blastomere culture medium (Shelton and Bowerman, 1996).

Microscopy

Mounting embryos—OID embryos were mounted in blastomere culture media (Shelton and Bowerman, 1996) by hanging drop to relieve osmotic and mechanical pressures. A toxicity effect (Siomos et al., 2001) was avoided by removing bacteria and the mother carcass. Wild-type meiosis I embryos develop to hatching in these mounting conditions.

TEM—Animals were prepared for TEM as described previously (Poteryaev et al., 2005), without gluteraldehyde fixation and also imaged with a Phillips CM 120 (FEI, Hillsboro, OR) at 80 kV, with a Soft Imaging Systems (Lakewood, CO) CCD camera and software, and a Tecnai T12 (FEI, Hillsborough, OR, USA) at 80 kV, with an ES500W CCD camera and software from Gatan (Pleasanton, CA, USA).

Live cell imaging—Multiphoton laser-scanning microscopy (MPLSM) was done at LOCI (http://www.loci.wisc.edu) with a custom-designed multiphoton laser scanning optical workstation (Wokosin et al., 2003). This system uses a Nikon Eclipse TE300 inverted microscope with a Nikon VC 60X Plan Apo oil-immersion lens (NA 1.2) and 5W mode-locked Ti:sapphire laser (Spectra-Physics-Millennium/Tsunami) with excitation at 890 nm. The intensity data were collected by a H7422 PMT (Hamamatsu) and the transmitted signal was collected by a transmitted photodiode detector (Bio-Rad, Hercules, CA, USA). Image acquisition was done with WiscScan (http://www.loci.wisc.edu/wiscscan/). A Swept Field Confocal system (Prairie Technologies Inc, Middleton, WI, USA) with 488, 514 and 568 nm excitation lines was utilized with a Nikon Eclipse TE300 Microscope, 100× Superfluor Lens NA 1.4 (Nikon, Melville NY) and a Dual-View beam splitter (Roper Scientific, Tucson, AZ, USA) utilizing a FITC/Texas Red emission set. Fixed samples were imaged using a Bio-Rad MRC 1024 confocal microscope (Hercules, CA, USA). To quantify degranulation, MPLSM was done with similar settings (which preserve embryo viability for over 2000 scans) and vesicle fusion events were manually counted. Images were analyzed in ImageJ v1.37p (Abramoff et al., 2004), and results were recounted on several data sets using the point picker plugin. Images were processed in Photoshop v8.0 (Adobe Systems) using Gaussian blur to reduce noise, and levels and curves to enhance contrast of the object of interest.

Statistics

Statistical calculations of mean, standard deviation and *P*-value were determined by fitting a one-way ANOVA model with SAS 9.1.3 on measurements gathered from individual embryos.

RESULTS

Identification of cortical granules

Cortical granules in oocytes of other organisms readily stain with lectins (Hoodbhoy and Talbot, 2001), which bind sugar molecules of glycosylated proteins. To obtain evidence that *C. elegans* oocytes contain cortical granules, we stained them with a panel of fluorescent-labeled lectins. Several lectins stained the vitelline layer, cytoplasmic vesicles and 1 μm vesicles at the cortex of oocytes and embryos in meiosis I (see Fig. S1A–F in the supplementary material). Wheat germ agglutanin (WGA), used to identify cortical granules in human oocytes (Talevi et al., 1997), labeled 1 μm vesicles in *C. elegans* oocytes and meiosis I embryos, but not in older embryos (Fig. 1A–C). Eggshell labeling with WGA appeared brighter in older embryos, suggesting that it recognized a glycoprotein cargo of cortical granules that incorporates into the eggshell. The endoplasmic reticulum (ER) reorganizes into a reticulate structure in the cortex around the time of fertilization (Poteryaev et al., 2005). We found that domains of the reticulate ER were closely associated with cortical granules in clusters during prometaphase I (see Fig. S1G–I in the supplementary material) that were redistributed evenly across the cortex during metaphase I (Fig. 1D–F). Therefore, we conclude that *C. elegans* contains cortical granules that undergo dynamic trafficking similar to that of other organisms (Sardet et al., 2002).

We generated transgenic animals expressing a GFP fusion with ZK370.7: a protein with sequence homology to transmembrane nucleotide-sugar transporters, predicted to transport UDP-galactose. This putative Golgi marker (hereafter referred to as UGTP-1::GFP) labeled cytoplasmic puncta and large 1 μm vesicles in oocytes and young embryos, which were present for a narrow time window after fertilization. These vesicles were clustered in early prometaphase I, redistributed within the cortex and lost by the end of meiosis I (Fig. 1G–I). We found that UGTP-1::GFP co-localized with WGA-stained vesicles (Fig. 1J–L), indicating that it is packaged into cortical granules. The observation that cortical granules contain UGTP-1::GFP suggests that they may be Golgi-derived. CAV-1::GFP, a GFP fusion to caveolin, was previously shown to undergo trafficking consistent with cortical granule exocytosis (Sato et al., 2006), and also localizes to WGA-stained cortical granules more specifically than UGTP-1::GFP (see Fig. S1J–L in the supplementary material). Therefore, UGTP-1::GFP and CAV-1::GFP are convenient markers for live cell imaging of cortical granule trafficking.

We used transmission electron microscopy (TEM) and observed a unique population of vesicles present in oocytes. Oocytes are fertilized approximately every 23 minutes (McCarter et al., 1999), so that the age of each embryo can be inferred by its position within the uterus (see Fig. 4A). A mature oocyte contained a large number of vesicles closely associated with the reticulated ER (Fig. 2A). These approximately 1 μm vesicles had an

unusual morphology reminiscent of the ‘refringent granules’ shown to contribute to eggshell formation in other nematode species (Foor, 1967). Prometaphase I embryos contained reticulate ER interlaced with clusters of heterogeneous vesicles near the cortex (Fig. 2B). Metaphase I embryos contained the 1 μm vesicles dispersed throughout the cortex in close association with ER (Fig. 2C). These results are similar to our observations with lectin staining. We were unable to capture an embryo during degranulation, but we anticipate that the vesicles dock at the plasma membrane and are subsequently exocytosed based on our observations with the light microscope (see below). Consistent with this interpretation, embryos at meiosis II or older did not contain the 1 μm vesicles (Fig. 2D). These observations suggest that the 1 μm vesicles are cortical granules and that they may contribute to eggshell formation.

Cortical granule exocytosis occurs during anaphase I

In attempt to observe the rapid process of degranulation, we imaged embryos using swept field confocal (SFC) microscopy (Prairie Technologies, Middleton, WI, USA) to acquire images every 200 milliseconds. Embryos expressing histone::GFP (Praitis et al., 2001) were mounted with optimized techniques to preserve viability (see Materials and methods), labeled with the plasma membrane dye FM2–10 and imaged by SFC (Fig. 3; see Movie 1 in the supplementary material). Interestingly, exocytosis began shortly after the homologous chromosomes separated during anaphase I in the region near the meiotic spindle (Fig. 3B). Fused vesicles incorporated FM2–10 and appeared as pockets outlined with fluorescence. As anaphase I proceeded, a wave of exocytosis spread across the cortex (Fig. 3B–D,F), and a gap opened between the vitelline layer and the plasma membrane near the polar body (Fig. 3E). The size of the vesicle cavity ranged from 0.2 to 1.5 μm, consistent with the size of cortical granules we observed by lectin staining and TEM.

To analyze secretion, we developed a correlative imaging technique using MPLSM. We simultaneously acquired transmitted bright-field and fluorescence images by MPLSM. Embryos labeled with either FM2–10 or a fluorescent dextran dissolved in the culture medium indicated vesicle-fusion events in the fluorescent image (Fig. 3F), which appeared coincident with cup-shaped plasma membrane invaginations in the bright-field image (see Movies 2 and 3 in the supplementary material). These observations demonstrate that the focal perturbations of the plasma membrane visualized in the bright-field image correlate with secretory events observed with plasma membrane and extracellular media labels and can serve as a marker for exocytosis.

To determine whether the wave of secretion during anaphase I represented the exocytosis of cortical granules, we observed the loss of UGTP-1::GFP-labeled vesicles using correlative MPLSM imaging. Loss of UGTP-1::GFP-labeled vesicles coincided with the appearance of plasma membrane perturbations visible in the bright-field image (see Movie 4 in the supplementary material). We also observed the loss of UGTP-1::GFP-labeled vesicles in the presence of extracellular fluorescent dextran (see Movie 5 in the supplementary material). In this experiment the signal of the extracellular dextran was saturating, whereas the UGTP-1::GFP signal was significantly weaker. Therefore, the exchange of vesicle contents with extracellular buffer after exocytosis resulted in a dramatic increase in fluorescence in

the fused vesicle cavity. We also imaged the fusion of CAV-1::GFP-labeled vesicles to the plasma membrane in the presence of the plasma membrane dye FM4–64. The fluorescent signal from CAV-1::GFP is bright enough to image using SFC and capture two channels simultaneously. FM4–64 photobleached quickly and caused a toxicity effect when imaged by SFC with the 488 nm laser (not observed with FM2–10, data not shown), but allowed us to capture short movies. After fusion, the vesicle cavity was immediately labeled with FM4–64 and co-localized with CAV-1::GFP, which remained on the cytoplasmic side of the plasma membrane (see Movie 6 in the supplementary material). These results demonstrate that cortical granule exocytosis occurs during anaphase I.

OID proteins regulate cortical granules

Cortical granule exocytosis is required for the development of a polyspermy barrier on oocytes of other species (Wessel et al., 2001), therefore we hypothesized that it may contribute to formation of the eggshell in *C. elegans*. Inactivation of genes that lead to eggshell permeability cause the OID phenotype (Kaitna et al., 2002; Rappleye et al., 1999; Siomos et al., 2001). Many of the OID genes encode proteins either known or predicted to be involved in protein trafficking through the ER and Golgi. A number of cell cycle regulators also give rise to OID when depleted from the embryo. To gain further insight into the mechanisms that regulate cortical granule exocytosis and determine if this process is involved in eggshell formation, we assessed the fate of cortical granules following RNAi depletion of a selection of OID genes representing these functional categories. Each gene was tested in both the UGTP-1::GFP and CAV-1::GFP transgenic lines (see Table 1).

Our results are consistent with the hypothesis that secretion of cortical granule proteoglycan cargo is required for eggshell formation. Previous results showed that depletion of SAR-1 (ZK180.4 – WormBase), a small GTPase required for anterograde transport from the ER, prevented formation of cortical granules (Sato et al., 2006). The syntaxin SYN-4 is required for vesicle fusion and is needed for eggshell formation and cytokinesis (Jantsch-Plunger and Glotzer, 1999). *syn-4(RNAi)* oocytes had abnormal populations of vesicles, sometimes accumulated at the plasma membrane (see Fig. S2E,F in the supplementary material). Eggshell chitin is generated by the chitin synthase, CHS-1 (Zhang et al., 2005), a putative cargo protein. Oocytes and embryos in *chs-1(RNAi)* animals showed no obvious change in cortical granule trafficking (Fig. 3C). Depletion of the redundant CPG-1 and CPG-2 chitin-binding chondroitin proteoglycans, also putative cargo proteins, and the glycosylation enzyme, SQV-4, reduced the size, but not the trafficking of cortical granules (see Fig. S2J,K in the supplementary material). CPG-1/-2 and SQV-4 may therefore be required to generate a significant mass of the proteoglycan cargo (the protein core and glycosyl side chains, respectively) secreted through cortical granule exocytosis for deposition of the eggshell.

The finding that membrane-trafficking regulators, but not putative cargo proteins, were required for cortical granule trafficking was not surprising. However, it was less clear how cell cycle regulatory genes might affect cortical granules. Therefore, we tested the effect of RNAi-depletion of several cell cycle OID proteins on cortical granule trafficking. First, we analyzed regulators that control the overall timing of cell division. Precocious CDK-1 activation occurs with *wee-1.3(RNAi)*, resulting in premature oocyte maturation (Burrows et

al., 2006). *wee-1.3(RNAi)* oocytes had large aggregates of UGTP-1::GFP-labeled puncta in the cytoplasm, which obscured the cortical granule population (see Fig. S2A in the supplementary material). CAV-1::GFP appeared normal in oocytes depleted in WEE-1.3, although in some cases vesicles moved to the cortex prematurely (see Fig. S2B in the supplementary material). Timely entry into mitosis requires the active CDK complex. Depletion of the primary M-phase CDK, CDK-1, caused retention of cortical granules in arrested embryos (see Fig. S2H in the supplementary material). To test the specificity of these effects, we depleted the CDK CKS-1 subunit by RNAi, which causes cytokinesis failures and delayed exit from mitosis, but not OID (Polinko and Strome, 2000). As expected, cortical granule trafficking appeared normal in *cks-1(RNAi)* embryos (see Fig. S2L in the supplementary material). These data indicate that only a subset of genes that regulate global cell cycle progression impact the trafficking of cortical granules.

A striking correlation exists between inhibiting genes that regulate progress through the metaphase to anaphase transition and the OID phenotype. *czw-1* is homologous to the ZW10 spindle assembly checkpoint component (Karess, 2005), implicated in regulation of vesicle trafficking (Hirose et al., 2004). *czw-1(RNAi)* caused UGTP-1::GFP to localize in enlarged puncta and smaller cytoplasmic vesicles (see Fig. S2C in the supplementary material). CAV-1::GFP was observed in small cytoplasmic vesicles (see Fig. S2D in the supplementary material), indicating that CZW-1 may regulate biogenesis of cortical granules. RNAi of APC/C subunits leads to cell cycle arrest in metaphase I (Shakes et al., 2003) and causes retention of CAV-1::GFP-labeled vesicles (Sato et al., 2006). We noticed that *apc-2(RNAi)* embryos retained clusters of cortical granules, reminiscent of wild-type prometaphase I embryos (Fig. 4D). The RNAi depletion of the *cyk-3* deubiquitination enzyme causes OID and cytokinesis failures (Kaitna et al., 2002), and might disrupt ubiquitin-mediated regulation of the cell cycle or membrane trafficking. *cyk-3(RNAi)* embryos retained clusters of cortical granules, similar to *apc-2(RNAi)* (see Fig. S2G in the supplementary material). These results suggest that the redistribution of cortical granules throughout the cortex is an ubiquitin-regulated process linked to the cell cycle and that regulators of the metaphase to anaphase transition also control trafficking of cortical granules.

To gain further insight into the cell-cycle regulation of degranulation, we investigated the role of an important downstream effector of APC/C in cortical granule exocytosis: separase. Inactivation of separase causes cytokinesis failures and delayed progression through mitosis, similar to *cks-1* (also known as *dom-6* – WormBase). However, in contrast to *cks-1*, separase inactivation also causes OID. Consistent with this phenotype, we found that cortical granules were retained in older embryos after depletion of separase (SEP-1) (Fig. 4E) or its inhibitory chaperone, securin (IFY-1) (see Fig. S2I in the supplementary material). To pursue these observations further, we examined embryos from an APC/C mutant [*mat-1(ye121)*] and from *sep-1(RNAi)* animals by TEM. APC/C mutant embryos were arrested in a meiotic state and contained cortical granules (Fig. 5A). *sep-1(RNAi)* embryos were not arrested but still retained cortical granules (Fig. 5B).

We compared the ultrastructure of the eggshell in wild-type, APC/C mutant and *sep-1(RNAi)* embryos. In the wild type, oocytes lacked an obvious covering (data not shown), but embryos in meiosis I contained cortical granules and had a single covering that

is likely to be the raised vitelline layer (Fig. 5C). In older embryos without cortical granules (i.e. putative post-degranulation), a three-layered eggshell was observed (Fig. 5D), similar to previous results (Rappleye et al., 1999). APC/C mutant (Fig. 5E) and *sep-1(RNAi)* embryos (Fig. 5F) only had a single covering, similar to immature wild-type eggshells. Therefore, the formation of an impermeable three-layered eggshell requires secretion of cortical granule cargo, a process that is regulated by APC/C, separase and probably other OID genes.

sep-1 mutations and RNAi impair cortical granule exocytosis

The observation that inactivation of a subset of cell cycle regulatory genes caused the retention of cortical granules suggests that a specific regulatory pathway controls their exocytosis. Separase stood out among these genes because it is an important regulator of anaphase, the time when degranulation occurs. To investigate whether separase regulates degranulation, we measured the extent and kinetics of exocytosis during anaphase I. We monitored the progress of anaphase I by measuring the rate of homologous chromosome separation and counted the number of exocytic events observed in a single focal plane of histone::GFP expressing embryos labeled with FM2–10. In wild-type embryos, secretion begins 92±8 seconds (n=5 embryos) after the chromosomes initiate separation at 20°C, and 72±9 seconds (n=7 embryos) at 25°C. The exocytic wave occurs during the middle of anaphase before the polar body is extruded (Fig. 6C–E), and takes 121±6 seconds to complete (n=7 embryos) at 20°C, and 76±10 seconds (n=7 embryos) at 25°C. We observed 57±7 (n=7 embryos), and 59±7 (n=10 embryos) exocytic events during anaphase I at 20°C and 25°C, respectively (Fig. 6A,B).

We next analyzed the dynamics of degranulation in *sep-1(RNAi)* and *sep-1(e2406)* mutant embryos. Animals fed *sep-1(RNAi)* for 17 to 20 hours at 25°C displayed chromosome nondisjunction and dramatically delayed anaphase completion (Fig. 6B,F–H), consistent with *sep-1* playing a role in CDK inhibition as observed in other species (Gorr et al., 2006). In addition, exocytosis was significantly reduced (34±7 events, $P<10^{-4}$, n=9 embryos, Fig. 6A,B), the anaphase spindle was disorganized and polar body extrusion failed (Fig. 6F–H). Surprisingly, *sep-1(e2406)* embryos entered anaphase without severe chromosome nondisjunction after 12 to 14 hours at 25°C (Fig. 6B), but only 26±6 exocytic events were observed ($P<10^{-4}$, n=9 embryos) (Fig. 6A,B). The reduced chromosome separation observed in *sep-1(e2406)* embryos during late anaphase (Fig. 6I,J) may be due to steric hindrance of polar body extrusion by the limited gap between the vitelline and plasma membrane and by the mislocalization of separase (see below). In some *sep-1(e2406)* embryos, a furrow enclosed the chromosomes at the cortex despite the reduced gap (Fig. 6K). In summary, both *sep-1(RNAi)* and *sep-1(e2406)* embryos have a similar reduction of cortical granule exocytosis, but *sep-1(RNAi)* shows much stronger cell cycle delays, more severe chromosome nondisjunction, spindle and polar body extrusion defects. Therefore, *sep-1(e2406)* is a hypomorphic allele that is compromised for a subset of the multiple distinct functions of separase.

As a control, we measured cortical granule exocytosis during anaphase in *cks-1(RNAi)* embryos, which have cell cycle delays and cytokinesis failures similar to those of separase mutants, but are not OID. We also analyzed *chs-1(RNAi)* embryos, which are OID because

they lack chitin in the eggshell (Zhang et al., 2005). In both cases degranulation occurred normally (Fig. 6A). The spindle of *cks-1(RNAi)* embryos did not undergo the normal rotation and movement observed in the wild type (Yang et al., 2005), the distance that chromosomes separated during anaphase was reduced, and polar body extrusion failed (data not shown). However, after chromosomes separated, a normal wave of cortical granule exocytosis occurred (58±8 events, n=5 embryos, Fig. 6A). *chs-1(RNAi)* embryos failed polar body extrusion, but cortical granule exocytosis occurred normally (56±8 events, n=3 embryos, Fig. 6A). The plasma membrane became deformed immediately after secretion (data not shown), possibly due to the improper organization of eggshell components in the absence of chitin. Together, these results demonstrate that anaphase failures do not universally inhibit degranulation and that not all OID phenotypes result from secretion failures. The observation that *sep-1(e2406)* embryos have relatively normal anaphase progression yet reduced cortical granule exocytosis suggests that separase may have a direct role in regulating this process.

Separase localizes to cortical granules during anaphase I

To examine further the role of separase in cortical granule exocytosis, we determined the localization of separase by expressing GFP::SEP-1 in oocytes and young embryos (Fig. 7A–F and see Movie 7 in the supplementary material) and by immunofluorescence with polyclonal antibodies directed against endogenous separase (Fig. 7G–I). During oocyte maturation, cytoplasmic separase rapidly accumulated in the nucleus on homologous chromosomes. Separase also localized to unusual filaments distributed throughout the cortex (Fig. 7A,B,H). Several proteins have been found in similar filaments in meiosis I embryos (Monen et al., 2005), and also in *Drosophila* oocytes (Gilliland et al., 2007). We found that separase co-localized in filaments with HIM-10 (Fig. 8A–C), the homologue of the kinetochore component nuf2 (Howe et al., 2001). Before anaphase onset, separase was lost from these filamentous structures and accumulated on cortical vesicles (Fig. 7C,G). Separase co-localized with WGA-labeled cortical granules during anaphase I (Fig. 8D–F). Separase-labeled vesicles were lost during anaphase I, beginning in the region near the meiotic spindle (Fig. 7G). We demonstrated that these vesicles undergo exocytosis by live cell imaging with correlative MPLSM and double-labeling with fluorescent dextran (see Movies 8 and 9 in the supplementary material). In mitotic embryos, separase localized to centrosomes, chromosomes and a diffuse cloud around the metaphase plate and anaphase spindle (Fig. 7E,F,I).

To obtain further insight into the *sep-1(e2406)* mutant phenotype, we localized the mutant SEP-1 protein by immunofluorescence in embryos incubated at 25°C for 11 hours. In the mutant, SEP-1 was still present on the anaphase I spindle (Fig. 8H,I), although it was reduced when compared with wild-type embryos. However, we did not detect the mutant protein on cortical granules during anaphase I (Fig. 8G–I). Therefore, the *sep-1(e2406)* allele appears to disrupt separase function partly through disrupting its localization to cortical granules. The observations that separase localizes to cortical granules and is required for degranulation suggests that separase could directly regulate exocytosis.

DISCUSSION

Cortical granule exocytosis in *C. elegans*

Cortical granule exocytosis is a phenomenon observed in the oocytes of many organisms (Wessel et al., 2001). We have identified cortical granules in *C. elegans* and have observed that degranulation occurs during anaphase I. We observed several steps of cortical granule trafficking and eggshell formation and identified a number of OID genes that perturb this process when inactivated (Fig. 9). Several cell cycle genes that cause OID are required for the exocytosis of cortical granules. In particular, separase localized to cortical granules during anaphase I and was required for degranulation (Fig. 9). It is possible that OID genes such as securin, spindle assembly checkpoint components and APC/C affect cortical granule exocytosis partly through regulation of separase.

It will be important to decipher the signals that trigger egg activation in *C. elegans*. Oocytes induced to mature by mutant sperm that are incapable of fertilization fail to complete anaphase I properly, do not form a proper eggshell and do not attempt meiosis II (McNally and McNally, 2005). Interestingly, cortical granules were still capable of fusing to the plasma membrane in unfertilized oocytes (Sato et al., 2006). As there is no discrete cell cycle arrest after maturation in *C. elegans* (McNally and McNally, 2005), unfertilized oocytes enter anaphase I. Entry into anaphase requires separase activation, which triggers degranulation. Further studies are required to understand the nature of the eggshell defect associated with unfertilized oocytes, and to know whether CGE is impaired. One possibility is that the wave of exocytosis may not occur with normal kinetics, disrupting eggshell formation. We hypothesize that signals possibly from both ovulation and fertilization stimulate an egg activation pathway acting upstream of, or in parallel with, separase to coordinate secretion of eggshell components with cell cycle progression in *C. elegans*.

Our data indicate that exocytosis of cortical granules is required for deposition of a mature three-layered eggshell in *C. elegans*. The outer vitelline layer, which covers oocytes, may function in sperm binding and restricting the free diffusion of cortical granule cargo, similar to its role in other species (Wessel et al., 2001). Interestingly, the vitelline envelope appears to separate from the plasma membrane at the time of fertilization, which could be part of a mechanism to prevent polyspermy. Our results also indicate that degranulation deposits the constituents of the inner two layers. Complex fibers made up of chitin and protein arranged in sheets have been observed in other nematodes (Wharton, 1980). We suspect that the chitin synthase, *chs-1*, glycosylation enzymes such as *sqv-4* and the *cpg-1/-2* proteoglycans are involved in eggshell layer formation (Herman et al., 1999; Hwang and Horvitz, 2002; Johnston et al., 2006; Olson et al., 2006; Zhang et al., 2005). As the *C. elegans* eggshell is permeable until late meiosis II, an elaborate process is probably involved in formation of mature eggshell. Further studies will be required to define how the secretions from the oocyte are assembled into the layers of the eggshell.

Secretion during anaphase

Our observations reveal that cortical granule exocytosis occurs during anaphase I and is regulated by separase. There are precedents for functions of separase outside cohesin

cleavage. For example, in budding yeast, separase plays a non-proteolytic role in the regulation of anaphase spindle dynamics (Higuchi and Uhlmann, 2005; Sullivan and Uhlmann, 2003), controls asymmetric spindle pulling forces (Ross and Cohen-Fix, 2004) and activates a signaling pathway that promotes exit from mitosis and cytokinesis (de Gramont and Cohen-Fix, 2005; Stegmeier et al., 2002). In frogs, separase plays a role in the centrosome duplication cycle (Tsou and Stearns, 2006). In the mouse, proteolytic-inactive separase can rescue polar body extrusion but not chromosome segregation in separase-knockout oocytes (Kudo et al., 2006). Separase is required for progression through meiosis in both mouse and frog oocytes in part because it binds and inhibits CDK (Gorr et al., 2005; Gorr et al., 2006). We have shown that separase localizes to cortical granules and loss of separase activity reduces exocytosis during anaphase I. Cortical granule exocytosis during anaphase I might create the necessary extracellular space, as well as provide additional membrane, for polar body extrusion. Consistent with this notion, inactivation of separase dramatically reduced the extracellular space near the polar body and restricted polar body extrusion (Fig. 6F–K). In *sep-1(e2406)* mutant embryos the initial separation of homologous chromosomes was essentially normal, but cortical granule exocytosis was still reduced. This is consistent with our observation that *sep-1(e2406)* mutant protein does not localize properly to cortical granules but retains some localization to chromosomes. These observations suggest that the *sep-1(e2406)* mutation might preferentially affect the role of separase in cortical granule exocytosis while retaining proteolytic activity toward cohesin. This suggestion is strengthened by the position of the *sep-1(e2406)* mutation (Siomos et al., 2001), which does not reside in the catalytic domain, but rather within a large N-terminal domain predicted to contain ARM repeats (Viadiu et al., 2005).

We observed rare cortical granule exocytic events during anaphase II in separase mutant and RNAi-depleted embryos (data not shown), further suggesting that cortical granule exocytosis is promoted specifically during anaphase. The observation that cell cycle regulatory genes control cortical granule exocytosis is surprising given observations made in other organisms. In *Xenopus*, inhibiting exit from mitosis by a non-degradable cyclin B did not prevent cortical granule exocytosis during egg activation (Murray et al., 1989). Although mouse oocytes can be parthenogenetically activated to undergo degranulation without cell cycle resumption (Ducibella et al., 2002), another study indicated that chromosome separation initiates before cortical granule exocytosis (Tombes et al., 1992). Studies in hamster oocytes indicated that limited exocytosis of cortical granules over the meiosis I spindle occurs during anaphase, contributing membrane for polar body extrusion (Okada et al., 1986). These data suggest that cortical granule exocytosis could also be regulated by separase during anaphase in oocytes of other organisms.

The finding that separase regulates cortical granule exocytosis during anaphase I leads us to speculate that separase may also regulate secretion during mitotic cell divisions. This control mechanism provides an elegant solution for synchronizing membrane trafficking during cell cleavage with chromosome segregation by linking these events through the activity of separase. We have observed multinucleate cells in *sep-1(e2406)* mutants shifted to the non-permissive temperature after eggshell formation (data not shown), suggesting that loss of separase activity can cause cytokinesis defects in mitotic divisions. It is well known that secretion is required during late anaphase and cytokinesis (Albertson et al., 2005), and

separase was identified in a screen for genes required for secretion (Bard et al., 2006). Further analysis of how separase promotes exocytosis during anaphase I, and whether it regulates cytokinesis by a similar mechanism should be a fertile focus of future studies.

Supplementary Material

Refer to Web version on PubMed Central for supplementary material.

Acknowledgments

We thank Kraig Kumfer for cloning bombardment vectors, Haining Zhang for staining protocols and other lab members for feedback; Peter Crump for statistical analysis and Leanne Olds for drawing illustrations; Bill Vogt, Willy Hausner and Mike Szulczewski of Prairie Technologies (Middleton, WI) for technical assistance with the swept-field Confocal; Bill Bement, Anna Skop, Bob Goldstein, Ji Liu and Francis Pelegri for sharing equipment, reagents and expertise. The Barbara Meyer lab graciously provided the HIM-10 antibody. cDNA clones were obtained from Yuji Kohara. This work is supported by the University of Basel to A.S., by the Intramural Research Program at the National Institutes of Health (NIH) National Institute of Diabetes and Digestive and Kidney Diseases to A.G. and C.R., a NIH grant (R01 GM7583) to J.W., a NIH SBIR grant (5R44MH065724) with Prairie Technologies to K.E. and a NIH training grant (5F32 GM076867-02) to J.B.

References

Abramoff MD, Magelhaes PJ, Ram SJ. Image Processing with ImageJ. Biophoton. Int. 2004; 11:36–42.

Albertson R, Riggs B, Sullivan W. Membrane traffic: a driving force in cytokinesis. Trends Cell Biol. 2005; 15:92–101. [PubMed: 15695096]

Bard F, Casano L, Mallabiabarrena A, Wallace E, Saito K, Kitayama H, Guizzunti G, Hu Y, Wendler F, Dasgupta R, et al. Functional genomics reveals genes involved in protein secretion and Golgi organization. Nature. 2006; 439:604–607. [PubMed: 16452979]

Brenner S. The genetics of *Caenorhabditis elegans*. Genetics. 1974; 77:71–94. [PubMed: 4366476]

Burrows AE, Sceurman BK, Kosinski ME, Richie CT, Sadler PL, Schumacher JM, Golden A. The *C. elegans* Myt1 ortholog is required for the proper timing of oocyte maturation. Development. 2006; 133:697–709. [PubMed: 16421191]

Chitwood, BG., Chitwood, MBH. Introduction to Nematology. Baltimore: University Park Press; 1974.

de Gramont A, Cohen-Fix O. The many phases of anaphase. Trends Biochem. Sci. 2005; 30:559–568. [PubMed: 16126387]

Ducibella T, Huneau D, Angelichio E, Xu Z, Schultz RM, Kopf GS, Fissore R, Madoux S, Ozil JP. Egg-to-embryo transition is driven by differential responses to Ca(2+) oscillation number. Dev. Biol. 2002; 250:280–291. [PubMed: 12376103]

Foor WE. Ultrastructural aspects of oocyte development and shell formation in Ascaris lumbricoides. J. Parasitol. 1967; 53:1245–1261. [PubMed: 6078612]

Gilliland WD, Hughes SE, Cotitta JL, Takeo S, Xiang Y, Hawley RS. The multiple roles of Mps1 in Drosophila female meiosis. PLoS Genet. 2007; 3:e113. [PubMed: 17630834]

Gonczy P, Schnabel H, Kaletta T, Amores AD, Hyman T, Schnabel R. Dissection of cell division processes in the one cell stage *Caenorhabditis elegans* embryo by mutational analysis. J. Cell Biol. 1999; 144:927–946. [PubMed: 10085292]

Gorr IH, Boos D, Stemmann O. Mutual inhibition of separase and Cdk1 by two-step complex formation. Mol. Cell. 2005; 19:135–141. [PubMed: 15989971]

Gorr IH, Reis A, Boos D, Wuhr M, Madgwick S, Jones KT, Stemmann O. Essential CDK1-inhibitory role for separase during meiosis I in vertebrate oocytes. Nat. Cell Biol. 2006; 8:1035–1037. [PubMed: 16906143]

Herman T, Hartwieg E, Horvitz HR. *sqv* mutants of *Caenorhabditis elegans* are defective in vulval epithelial invagination. Proc. Natl. Acad. Sci. USA. 1999; 96:968–973. [PubMed: 9927677]

Higuchi T, Uhlmann F. Stabilization of microtubule dynamics at anaphase onset promotes chromosome segregation. Nature. 2005; 433:171–176. [PubMed: 15650742]

Hirose H, Arasaki K, Dohmae N, Takio K, Hatsuzawa K, Nagahama M, Tani K, Yamamoto A, Tohyama M, Tagaya M. Implication of ZW10 in membrane trafficking between the endoplasmic reticulum and Golgi. EMBO J. 2004; 23:1267–1278. [PubMed: 15029241]

Hoodbhoy T, Talbot P. Characterization, fate, and function of hamster cortical granule components. Mol. Reprod. Dev. 2001; 58:223–235. [PubMed: 11139235]

Howe M, McDonald KL, Albertson DG, Meyer BJ. HIM-10 is required for kinetochore structure and function on *Caenorhabditis elegans* holocentric chromosomes. J. Cell Biol. 2001; 153:1227–1238. [PubMed: 11402066]

Hwang HY, Horvitz HR. The SQV-1 UDP-glucuronic acid decarboxylase and the SQV-7 nucleotide-sugar transporter may act in the Golgi apparatus to affect *Caenorhabditis elegans* vulval morphogenesis and embryonic development. Proc. Natl. Acad. Sci. USA. 2002; 99:14218–14223. [PubMed: 12391314]

Jantsch-Plunger V, Glotzer M. Depletion of syntaxins in the early *Caenorhabditis elegans* embryo reveals a role for membrane fusion events in cytokinesis. Curr. Biol. 1999; 9:738–745. [PubMed: 10421575]

Johnston WL, Krizus A, Dennis JW. The eggshell is required for meiotic fidelity, polar-body extrusion and polarization of the *C. elegans* embryo. BMC Biol. 2006; 4:35. [PubMed: 17042944]

Kaitna S, Schnabel H, Schnabel R, Hyman AA, Glotzer M. A ubiquitin C-terminal hydrolase is required to maintain osmotic balance and execute actin-dependent processes in the early *C. elegans* embryo. J. Cell Sci. 2002; 115:2293–2302. [PubMed: 12006614]

Kamath RS, Martinez-Campos M, Zipperlen P, Fraser AG, Ahringer J. Effectiveness of specific RNA-mediated interference through ingested double-stranded RNA in Caenorhabditis elegans. Genome Biol. 2001; 2 RESEARCH0002.

Kamath RS, Fraser AG, Dong Y, Poulin G, Durbin R, Gotta M, Kanapin A, Le Bot N, Moreno S, Sohrmann M, et al. Systematic functional analysis of the *Caenorhabditis elegans* genome using RNAi. Nature. 2003; 421:231–237. [PubMed: 12529635]

Karess R. Rod-Zw10-Zwilch: a key player in the spindle checkpoint. Trends Cell Biol. 2005; 15:386–392. [PubMed: 15922598]

Kudo NR, Wassmann K, Anger M, Schuh M, Wirth KG, Xu H, Helmhart W, Kudo H, McKay M, Maro B, et al. Resolution of chiasmata in oocytes requires separase-mediated proteolysis. Cell. 2006; 126:135–146. [PubMed: 16839882]

McCarter J, Bartlett B, Dang T, Schedl T. On the control of oocyte meiotic maturation and ovulation in *Caenorhabditis elegans*. Dev. Biol. 1999; 205:111–128. [PubMed: 9882501]

McNally KL, McNally FJ. Fertilization initiates the transition from anaphase I to metaphase II during female meiosis in *C. elegans*. Dev. Biol. 2005; 282:218–230. [PubMed: 15936342]

Monen J, Maddox PS, Hyndman F, Oegema K, Desai A. Differential role of CENP-A in the segregation of holocentric *C. elegans* chromosomes during meiosis and mitosis. Nat. Cell Biol. 2005; 7:1248–1255. [PubMed: 16273096]

Murray AW, Solomon MJ, Kirschner MW. The role of cyclin synthesis and degradation in the control of maturation promoting factor activity. Nature. 1989; 339:280–286. [PubMed: 2566918]

Musacchio A, Salmon ED. The spindle-assembly checkpoint in space and time. Nat. Rev. Mol. Cell Biol. 2007; 8:379–393. [PubMed: 17426725]

Nasmyth K. Segregating sister genomes: the molecular biology of chromosome separation. Science. 2002; 297:559–565. [PubMed: 12142526]

Okada A, Yanagimachi R, Yanagimachi H. Development of a cortical granule-free area of cortex and the perivitelline space in the hamster oocyte during maturation and following ovulation. J. Submicrosc. Cytol. 1986; 18:233–247. [PubMed: 3712508]

Olson SK, Bishop JR, Yates JR, Oegema K, Esko JD. Identification of novel chondroitin proteoglycans in *Caenorhabditis elegans*: embryonic cell division depends on CPG-1 and CPG-2. J. Cell Biol. 2006; 173:985–994. [PubMed: 16785326]

Peters JM. The anaphase promoting complex/cyclosome: a machine designed to destroy. Nat. Rev. Mol. Cell Biol. 2006; 7:644–656. [PubMed: 16896351]

Polinko ES, Strome S. Depletion of a Cks homolog in *C. elegans* embryos uncovers a post-metaphase role in both meiosis and mitosis. Curr. Biol. 2000; 10:1471–1474. [PubMed: 11102813]

Poteryaev D, Squirrell JM, Campbell JM, White JG, Spang A. Involvement of the actin cytoskeleton and homotypic membrane fusion in ER dynamics in *Caenorhabditis elegans*. Mol. Biol. Cell. 2005; 16:2139–2153. [PubMed: 15716356]

Praitis V, Casey E, Collar D, Austin J. Creation of low-copy integrated transgenic lines in *Caenorhabditis elegans*. Genetics. 2001; 157:1217–1226. [PubMed: 11238406]

Rappleye CA, Paredez AR, Smith CW, McDonald KL, Aroian RV. The coronin-like protein POD-1 is required for anterior-posterior axis formation and cellular architecture in the nematode *Caenorhabditis elegans*. Genes Dev. 1999; 13:2838–2851. [PubMed: 10557211]

Ross KE, Cohen-Fix O. A role for the FEAR pathway in nuclear positioning during anaphase. Dev. Cell. 2004; 6:729–735. [PubMed: 15130497]

Sardet C, Prodon F, Dumollard R, Chang P, Chenevert J. Structure and function of the egg cortex from oogenesis through fertilization. Dev. Biol. 2002; 241:1–23. [PubMed: 11784091]

Sato K, Sato M, Audhya A, Oegema K, Schweinsberg P, Grant BD. Dynamic regulation of caveolin-1 trafficking in the germ line and embryo of *Caenorhabditis elegans*. Mol. Biol. Cell. 2006; 17:3085–3094. [PubMed: 16672374]

Shakes DC, Sadler PL, Schumacher JM, Abdolrasulnia M, Golden A. Developmental defects observed in hypomorphic anaphase-promoting complex mutants are linked to cell cycle abnormalities. Development. 2003; 130:1605–1620. [PubMed: 12620985]

Shelton CA, Bowerman B. Time-dependent responses to *glp-1*-mediated inductions in early *C. elegans* embryos. Development. 1996; 122:2043–2050. [PubMed: 8681785]

Siomos MF, Badrinath A, Pasierbek P, Livingstone D, White J, Glotzer M, Nasmyth K. Separase is required for chromosome segregation during meiosis I in *Caenorhabditis elegans*. Curr. Biol. 2001; 11:1825–1835. [PubMed: 11728305]

Sonnichsen B, Koski LB, Walsh A, Marschall P, Neumann B, Brehm M, Alleaume AM, Artelt J, Bettencourt P, Cassin E, et al. Fullgenome RNAi profiling of early embryogenesis in *Caenorhabditis elegans*. Nature. 2005; 434:462–469. [PubMed: 15791247]

Stegmeier F, Visintin R, Amon A. Separase, polo kinase, the kinetochore protein Slk19, and Spo12 function in a network that controls Cdc14 localization during early anaphase. Cell. 2002; 108:207–220. [PubMed: 11832211]

Sullivan M, Uhlmann F. A non-proteolytic function of separase links the onset of anaphase to mitotic exit. Nat. Cell Biol. 2003; 5:249–254. [PubMed: 12598903]

Talevi R, Gualtieri R, Tartaglione G, Fortunato A. Heterogeneity of the zona pellucida carbohydrate distribution in human oocytes failing to fertilize in vitro. Hum. Reprod. 1997; 12:2773–2780. [PubMed: 9455851]

Tombes RM, Simerly C, Borisy GG, Schatten G. Meiosis, egg activation, and nuclear envelope breakdown are differentially reliant on Ca^{2+}, whereas germinal vesicle breakdown is Ca^{2+} independent in the mouse oocyte. J. Cell Biol. 1992; 117:799–811. [PubMed: 1577859]

Tsou MF, Stearns T. Mechanism limiting centrosome duplication to once per cell cycle. Nature. 2006; 442:947–951. [PubMed: 16862117]

Tunquist BJ, Maller JL. Under arrest: cytostatic factor (CSF)-mediated metaphase arrest in vertebrate eggs. Genes Dev. 2003; 17:683–710. [PubMed: 12651887]

Verbrugghe KJ, White JG. SPD-1 is required for the formation of the spindle midzone but is not essential for the completion of cytokinesis in *C. elegans* embryos. Curr. Biol. 2004; 14:1755–1760. [PubMed: 15458647]

Viadiu H, Stemmann O, Kirschner MW, Walz T. Domain structure of separase and its binding to securin as determined by EM. Nat. Struct. Mol. Biol. 2005; 12:552–553. [PubMed: 15880121]

Wessel GM, Brooks JM, Green E, Haley S, Voronina E, Wong J, Zaydfudim V, Conner S. The biology of cortical granules. Int. Rev. Cytol. 2001; 209:117–206. [PubMed: 11580200]

Wharton D. Nematode egg-shells. Parasitology. 1980; 81:447–463. [PubMed: 7003502]

Wokosin DL, Squirrell JM, Eliceiri KW, White JG. Optical workstation with concurrent, independent multiphoton imaging and experimental laser microbeam capabilities. Rev. Sci. Instrum. 2003; 74:193–201. [PubMed: 18607511]

Yamamoto I, Kosinski ME, Greenstein D. Start me up: cell signaling and the journey from oocyte to embryo in *C. elegans*. Dev. Dyn. 2006; 235:571–585. [PubMed: 16372336]

Yang HY, Mains PE, McNally FJ. Kinesin-1 mediates translocation of the meiotic spindle to the oocyte cortex through KCA-1, a novel cargo adapter. J. Cell Biol. 2005; 169:447–457. [PubMed: 15883196]

Zhang Y, Foster JM, Nelson LS, Ma D, Carlow CK. The chitin synthase genes *chs-1* and *chs-2* are essential for *C. elegans* development and responsible for chitin deposition in the eggshell and pharynx, respectively. Dev. Biol. 2005; 285:330–339. [PubMed: 16098962]

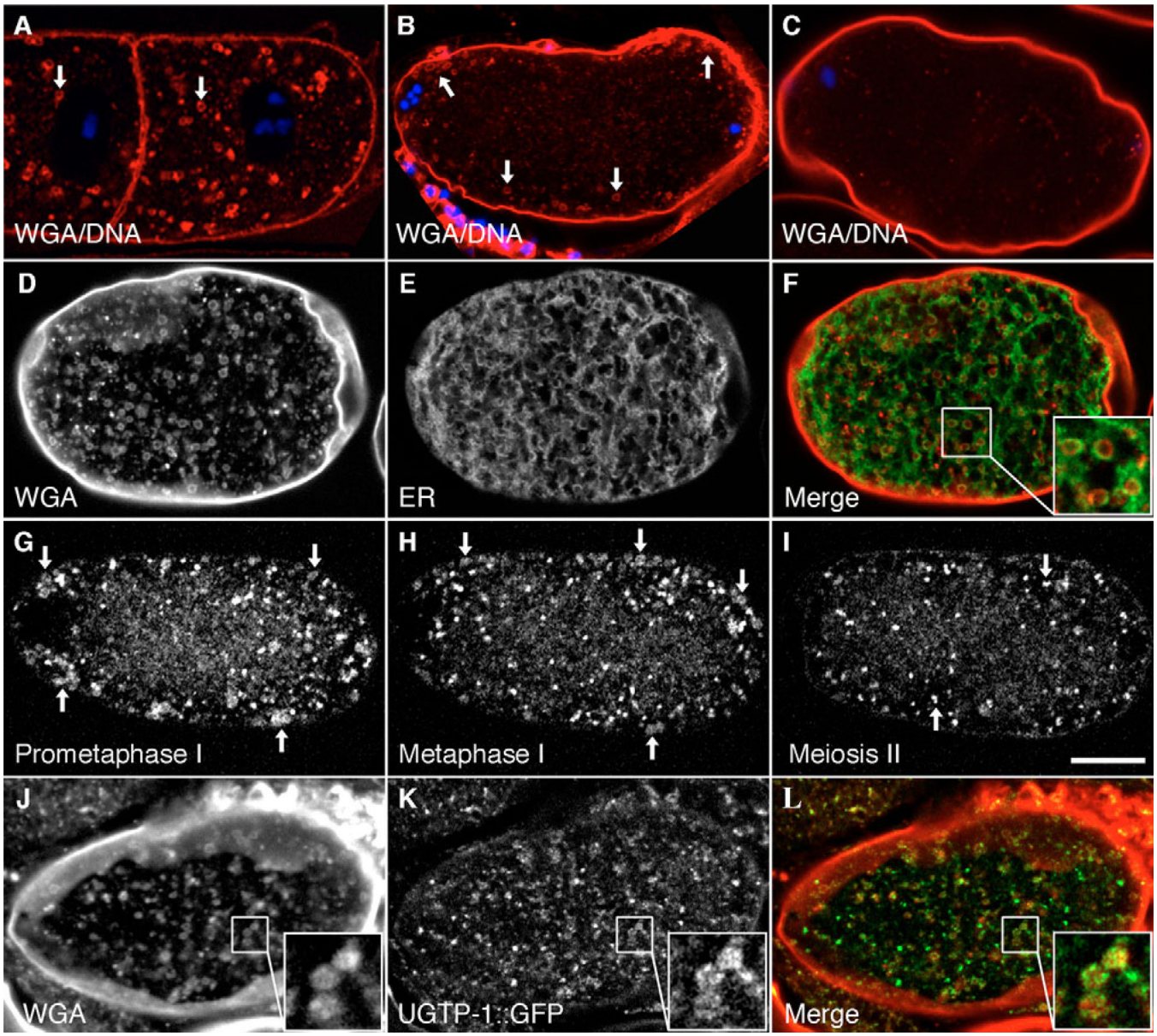

Fig. 1. Identification of cortical granules

(**A–C**) Succynilated WGA-labeled cortical granules in *C. elegans* oocytes (A), and prometaphase I embryos (B), but not in embryos after meiosis I (C) (DNA in blue). (**D–F**) WGA-labeled cortical granules (D) are associated with SP12::GFP-labeled reticulate ER (E) at the cortex of a metaphase I embryo; merge in F. (**G–I**) UGTP-1::GFP-labeled 1 μm vesicles were clustered in prometaphase I (arrows, G) and redistributed across the cortex by metaphase I (arrows, H). Smaller cytoplasmic puncta remain after loss of the 1 μm vesicles (arrows, I). (**J–L**) WGA staining (J) co-localized with UGTP-1::GFP (K) in cortical granules in the cortex of a metaphase I embryo; merge in L. Scale bar: 10 μm.

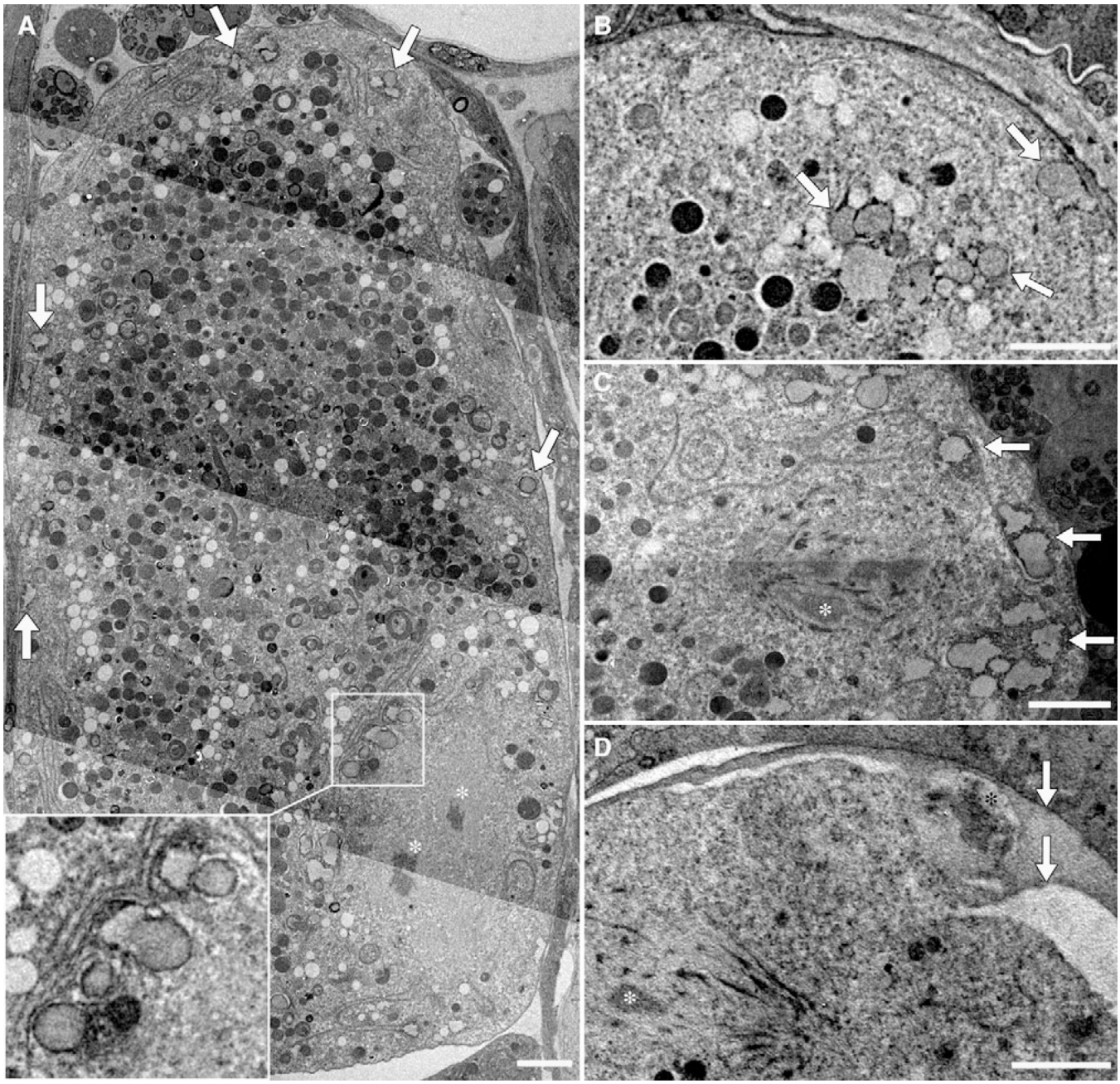

Fig. 2. TEM of cortical granules

(**A**) A mature *C. elegans* oocyte contains cortical granules (arrows); inset shows higher magnification of vesicles near the oocyte chromosomes (asterisks). (**B**) An embryo within the spermatheca contains a cortical granule near the plasma membrane (upper right arrow), and a cluster of heterogeneous vesicles (lower arrows). (**C**) A metaphase I embryo contains cortical granules (arrows) distributed across the cortex (asterisk denotes chromosome in spindle). The cortical granules are found in close association with reticulate ER (A–C). (**D**) Embryo at metaphase II (chromosome in spindle indicated by white asterisk) lacks cortical

granules, and the polar body (black asterisk) is trapped between eggshell layers (arrows). Scale bar: 2 μm.

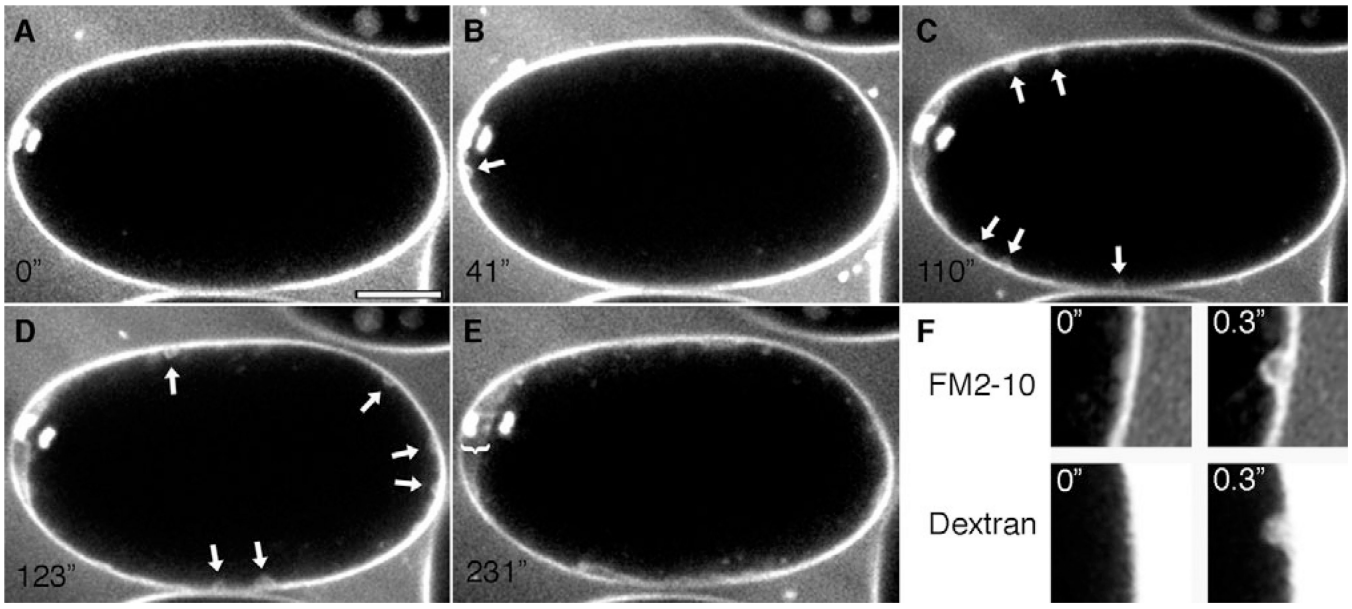

Fig. 3. A wave of exocytosis during anaphase I

C. elegans embryos expressing histone::GFP and labeled with the plasma membrane dye FM2–10 were imaged using SFC every 200 milliseconds. After the chromosome separation initiated (**A**), exocytic events (arrows) occurred near the spindle (**B**) and spread across the cortex (**C,D**) before the completion of anaphase I. Images in C and D are maximum projection summations of several frames in which a vesicle fusion event occurs. A gap is formed between the plasma membrane and the vitelline layer near the polar body (**E**, bracket). (**F**) Images of the plasma membrane before and after exocytosis, labeled with FM2–10 or a fluorescent dextran. Scale bar: 10 μm.

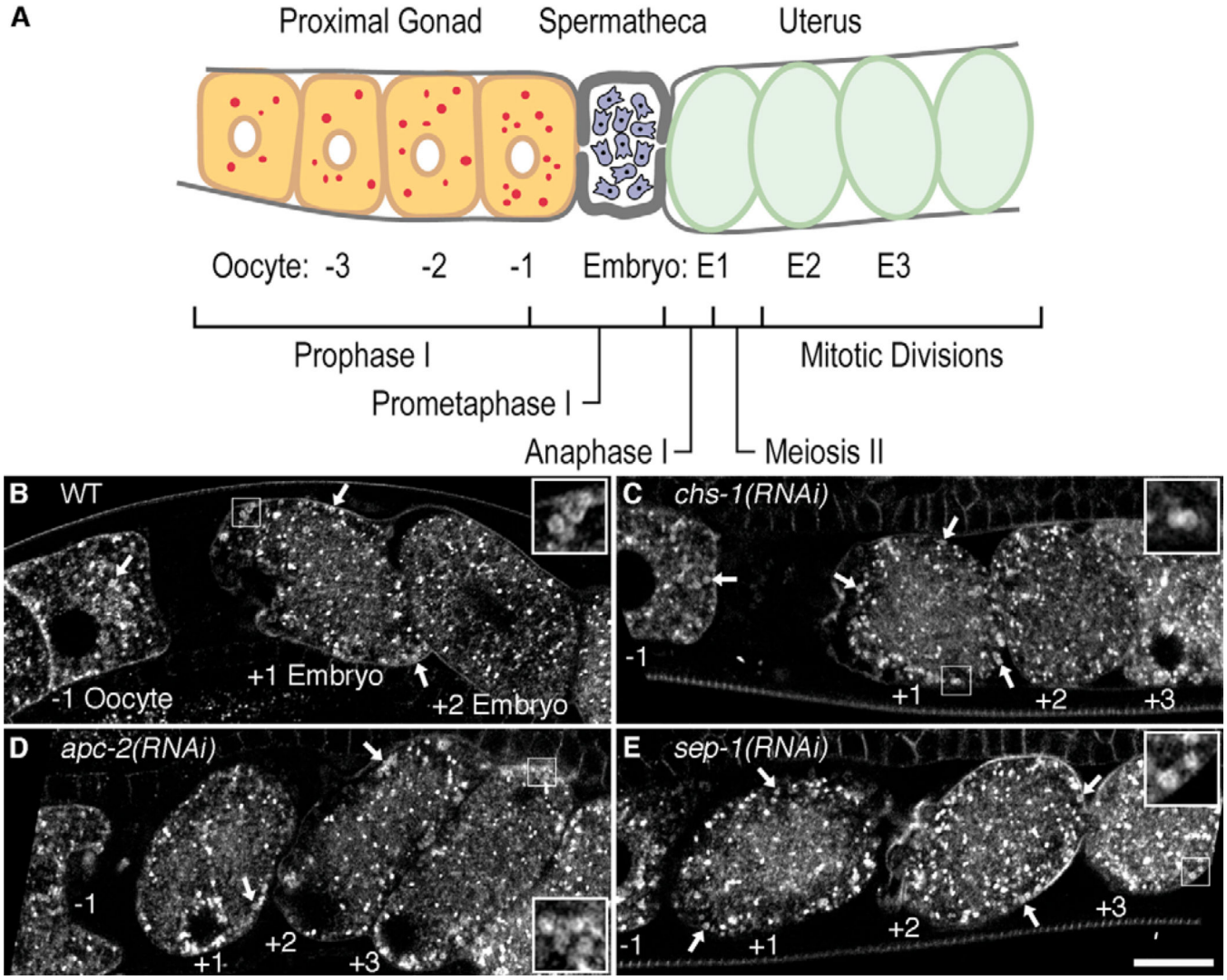

Fig. 4. RNAi of OID genes affects cortical granules

(**A**) Organization of the *C. elegans* gonad, showing approximate cell cycle stages based upon the position of oocytes and embryos in wild-type animals. (**B–D**) Cortical granules labeled with UGTP-1::GFP (indicated by arrows; insets show higher magnification of vesicles). In wild-type animals, embryo +1 was undergoing meiosis I and contains cortical granules, whereas embryo +2 was in the first mitotic division and lacks cortical granules. (C) *chs-1(RNAi)* oocytes and embryos showed the same UGTP-1::GFP pattern as the wild type. (D) *apc-2(RNAi)* caused retention of clustered UGTP-1::GFP-labeled cortical granules. (**E**) *sep-1(RNAi)* caused retention of UGTP-1::GFP-labeled cortical granules in the first three embryos. Scale bar: 10 μm.

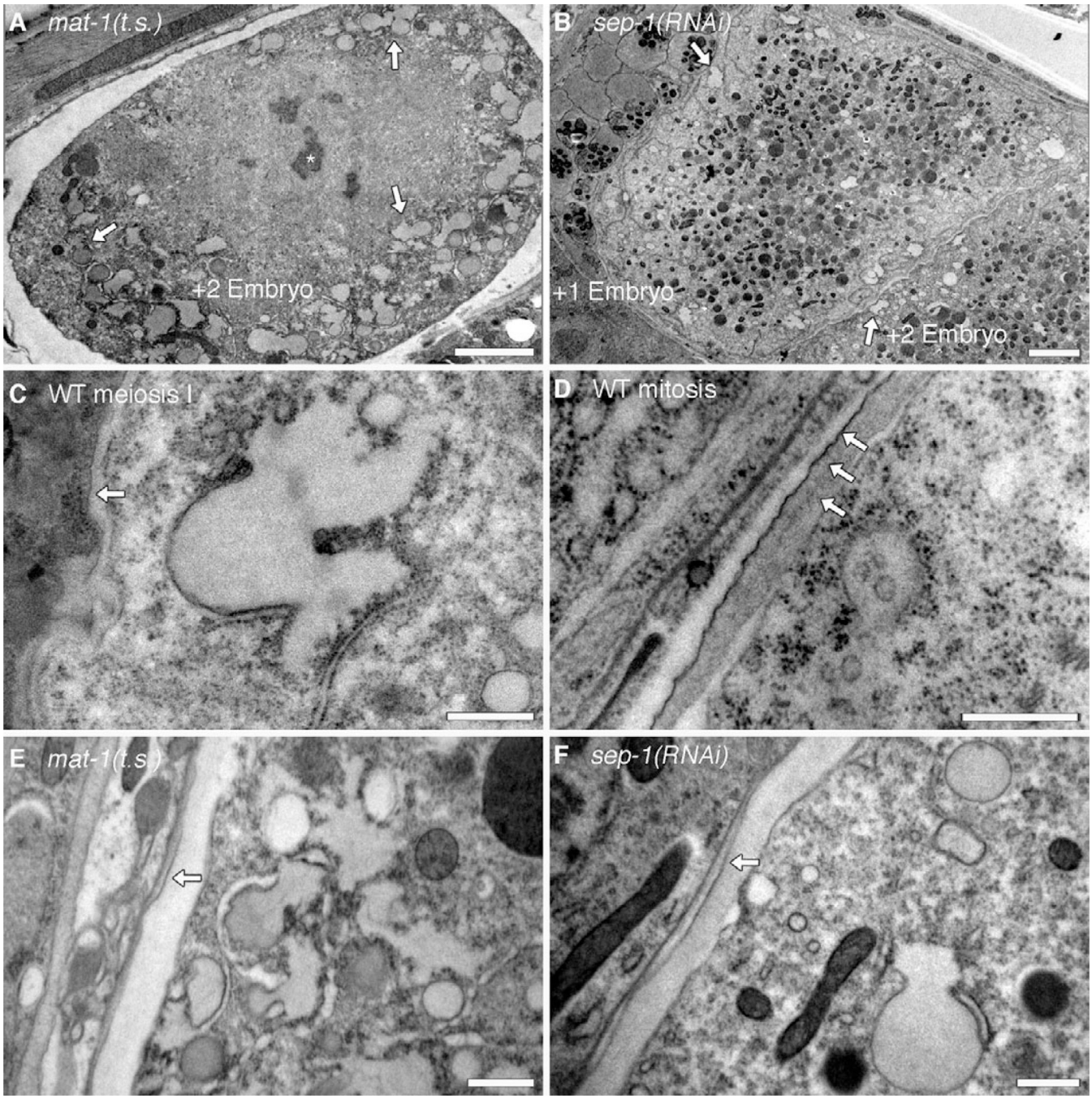

Fig. 5. TEM of APC/C mutant and *sep-1(RNAi)* embryos

(**A**) The +2 embryo in a *mat-1(ye121) C. elegans* did not exit meiosis (asterisk indicates chromosomes in meiotic spindle) and retained cortical granules (arrows). (**B**) *sep-1(RNAi)* embryos were not arrested, but retained cortical granules (arrows). (**C,D**) Comparison of eggshell structures. In wild-type meiosis I embryos that contain cortical granules, a single vitelline layer was present (C). In mitotic embryos, cortical granules were lost and a three-layer eggshell (arrows) structure was observed (D). The +2 embryo in APC/C mutant (**E**)

and *sep-1(RNAi)* (**F**) animals contained cortical granules and had a single vitelline layer (arrows), similar to immature wild-type eggshells. Scale bars: 3 μm in A,B; 0.5 μm in C–F.

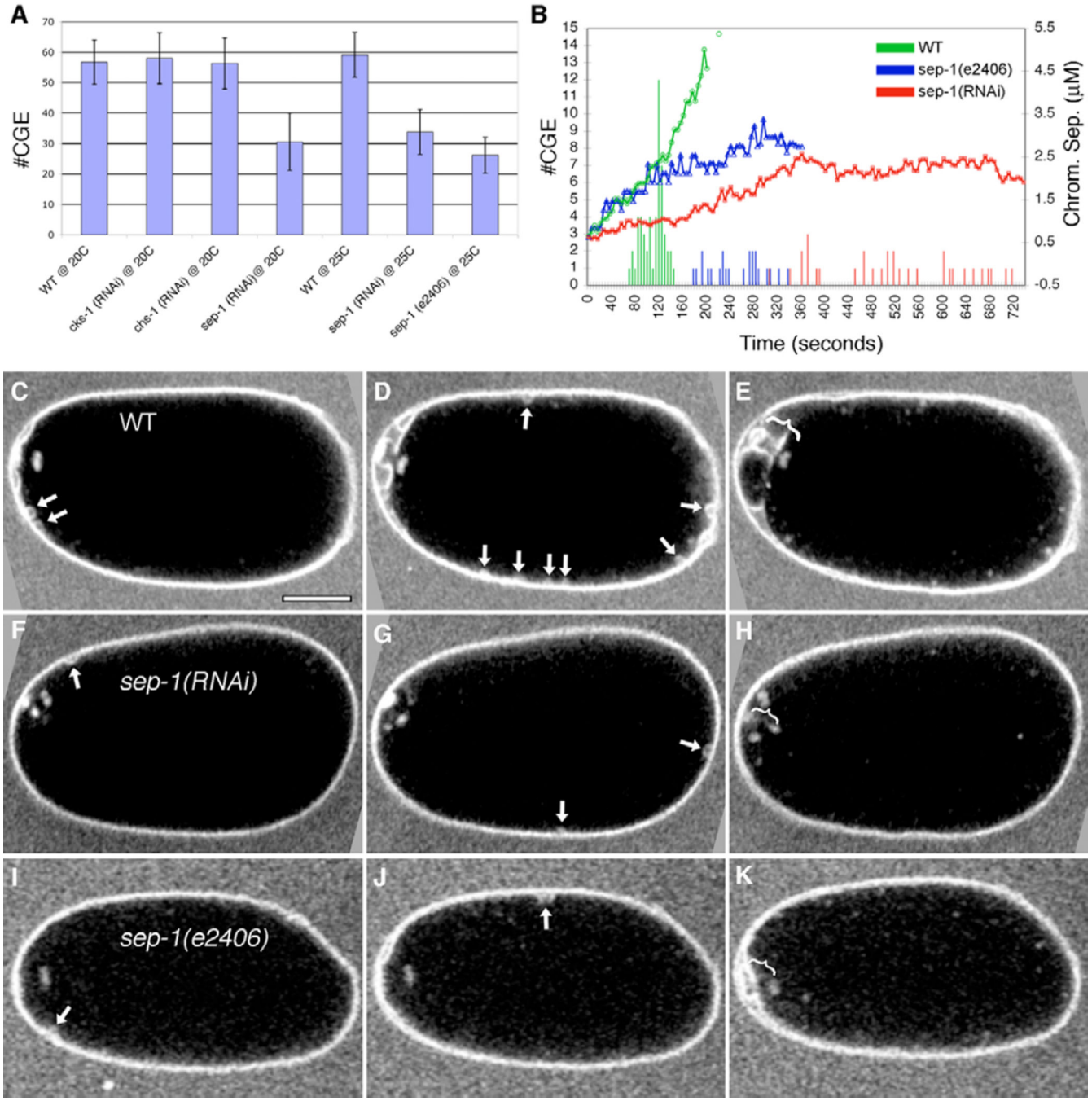

Fig. 6. The dynamics of the exocytic wave during anaphase I

C. elegans embryos labeled with histone::GFP and FM2–10 were imaged every 333 milliseconds using MPLSM. (**A**) Total exocytic events observed in wild-type, *chs-1(RNAi)* and *cks-1(RNAi)* embryos were nearly twice that of *sep-1(e2406)* and *sep-1(RNAi)* embryos. (**B**) Kinetic profiles of chromosome separation (plotted as a line) and exocytic events (columns) from single embryo recordings representative of average dynamics. Images from the movies are shown in **C–K**; brackets indicate distance measured between chromosomes, arrows indicate quantitated exocytic events. In wild type (green),

degranulation initiated after chromosomes separated by 1.5 μm, and completed before polar body extrusion. In *sep-1(RNAi)* (red), chromosome separation was severely reduced, the wave of exocytosis was reduced and took much longer. By contrast, in *sep-1(e2406)* embryos (blue) chromosomes initially separated normally, but still had a reduced level of exocytosis that began after chromosomes separated by 2.5 μm. Scale bar: 10 μm.

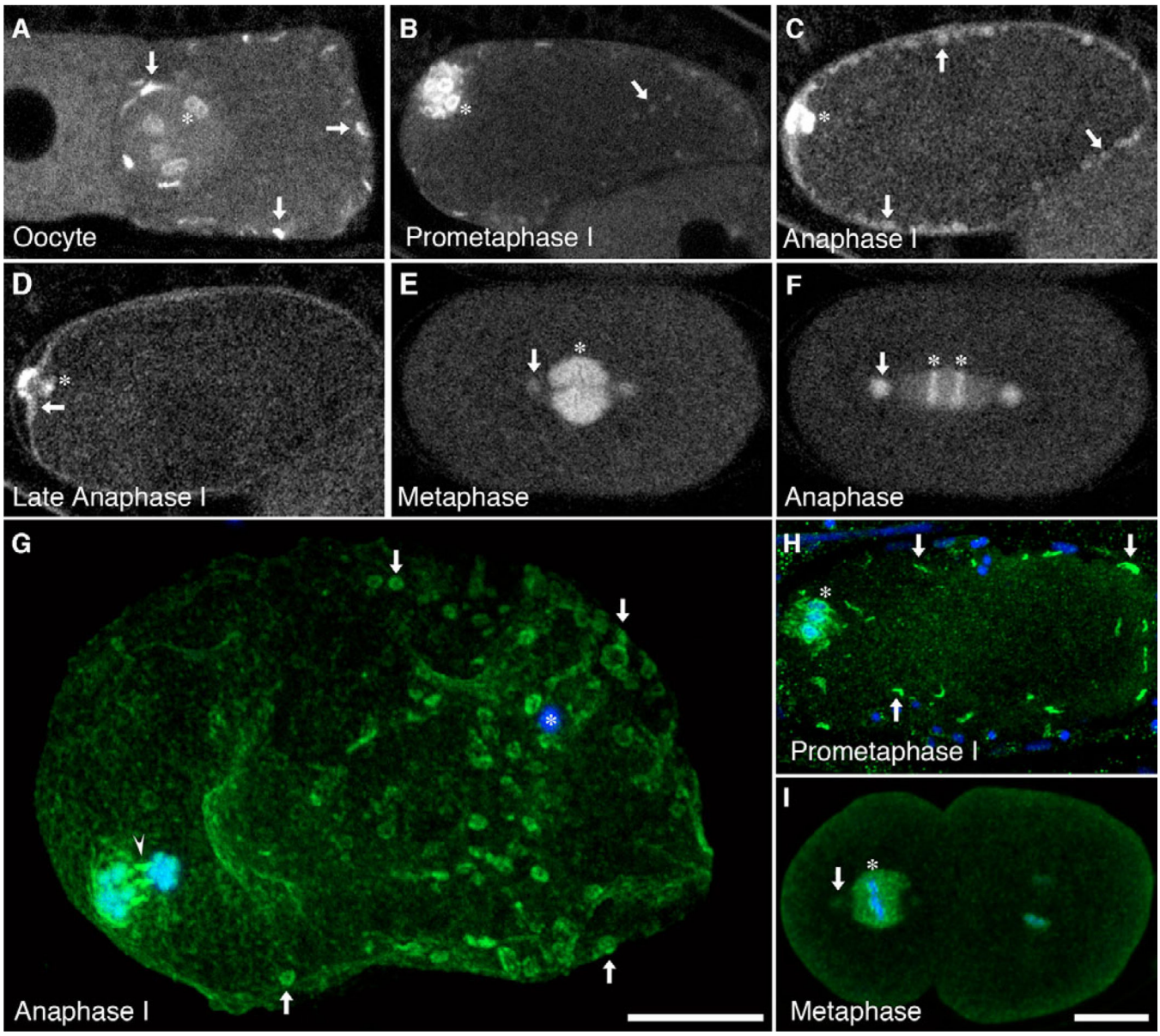

Fig. 7. Separase localizes to cortical granules in *C. elegans*

(**A**) Before ovulation, cytoplasmic GFP::SEP-1 rapidly accumulated in the nucleus, on chromosomes (asterisks) and cortical filaments (arrows). By metaphase I, GFP::SEP-1 was lost from filaments and appeared on cortical granules (**B,C**, arrows). GFP::SEP-1 disappeared during the exocytic wave in anaphase I and accumulated on the cortex near the polar body (**D**, arrow). (**E,F**) During mitosis, SEP-1::GFP localized to centrosomes (arrows), chromosomes (asterisks) and a diffuse cloud around the spindle. (**G–I**) Immunofluorescence with α-SEP-1 (green) and DNA (blue). (G) Separase-labeled vesicles (arrows) were absent from the vicinity of the spindle in an embryo that had partly completed the exocytic wave during anaphase I (maximum projection image). Separase localizes to six central spindle elements (arrowhead) between homologous chromosomes and accumulates on the cortex near the polar body (asterisk indicates sperm pronucleus). (H) During prometaphase I,

separase localized to filaments in the cortex (arrows) and in the spindle (asterisk). (I) Separase appeared on centrosomes (arrow) and chromosomes (asterisk) during mitosis. Scale bar: 10 μm.

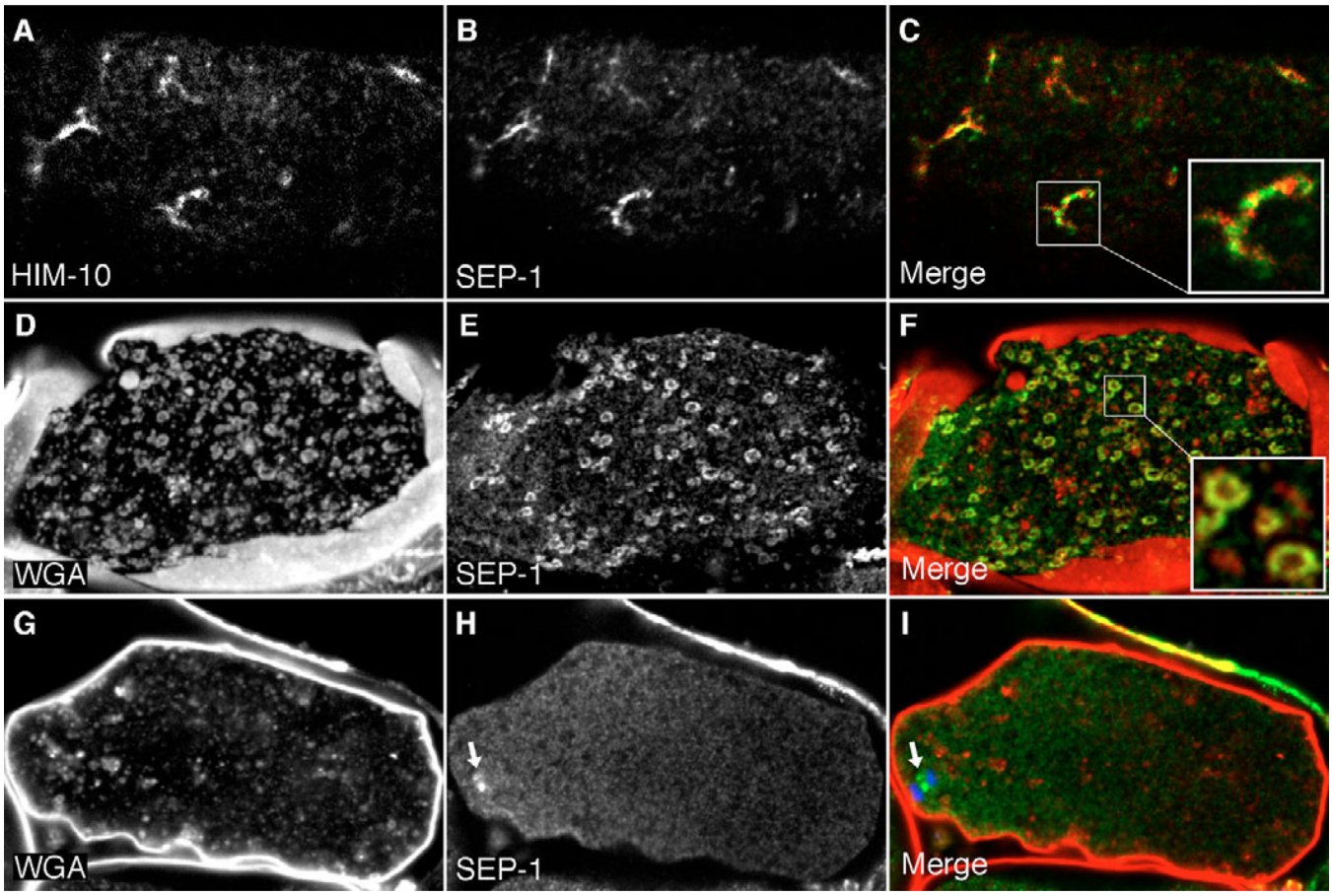

Fig. 8. Separase co-localization during meiosis I in *C. elegans*

During prometaphase I, the outer kinetochore protein, HIM-10 (**A**, red), co-localized in cortical filaments with separase (**B**, green); merge in (**C**). During anaphase I, cortical granules labeled with WGA (**D**, red) are also labeled with separase (**E**, green); merge in **F**, maximum projection image of four cortical planes. A *sep-1(e2406)* mutant embryo in anaphase I had cortical granules labeled with WGA (**G**, red) that were not labeled with separase antibody (**H**, green), although separase was still present but reduced on the anaphase spindle (arrow); merge in **I**. Scale bar: 10 μm.

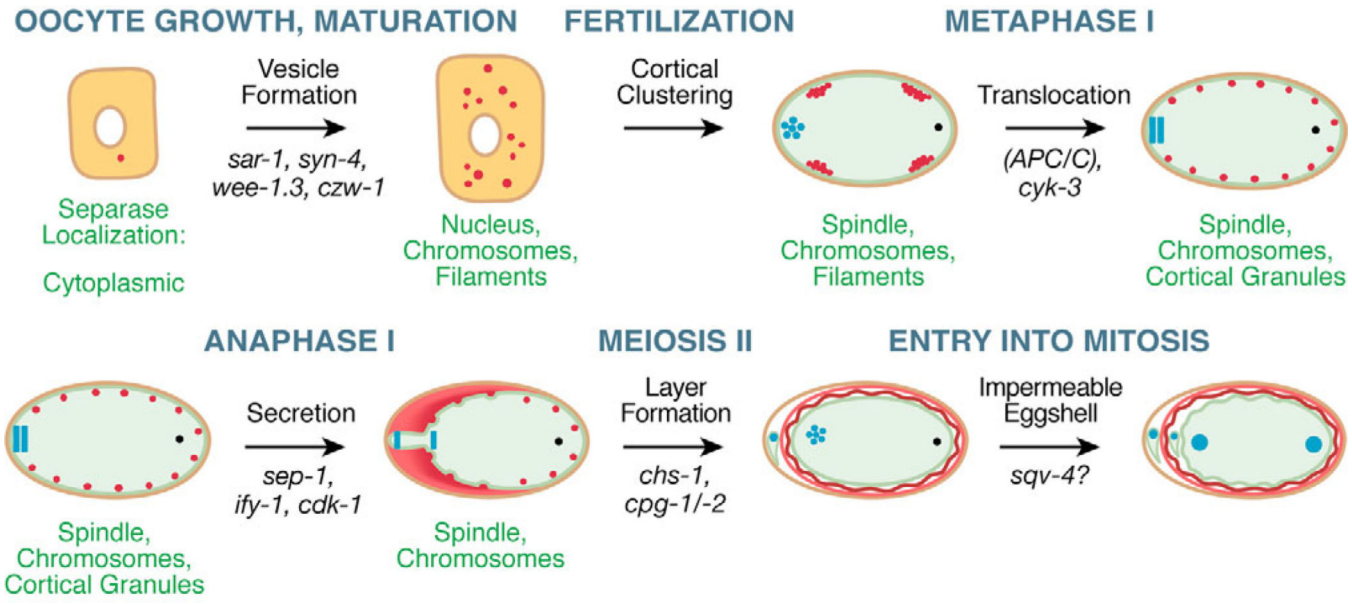

Fig. 9. Regulation of cortical granule trafficking in *C. elegans*

Depiction of several steps in cortical granule trafficking and eggshell formation, along with the OID genes involved. Separase localization is indicated. Immature oocytes form cortical granules (red) as they grow while separase remains in the cytoplasm. Just before ovulation, separase accumulates in the nucleus, on oocyte chromosomes (blue) and cytoplasmic filaments. The vitelline layer (brown) separates from the plasma membrane (green) around the time of fertilization (sperm pronucleus in black), and cortical granules cluster near the cortex. Separase is lost from filaments and accumulates on cortical granules as they redistribute in the cortex. Separase is lost during the wave of cortical granule exocytosis in anaphase I. Subsequently, the cargo of cortical granules assembles into the chitin (pink) and lipid (red) layers, which are permeable until late meiosis II.

Table 1

RNAi of OID genes disrupts cortical granule trafficking

RNAi	Class	Function	Oocytes	Embryo +1	Embryo +2
Control	–	–	Normal	Normal	Absent
wee-1.3	Cell cycle	CDK activation	UGTP-1 agg., normal CGs	Abnormal vesicles	Abnormal vesicles
czw-1	Cell cycle	SAC, membrane traffic	UGTP-1 puncta, small CGs	Abnormal vesicles	Abnormal vesicles
syn-4	Membrane traffic	Vesicle fusion	Vesicles at cortex	Abnormal vesicles	Abnormal vesicles
cyk-3	Cell cycle	Deubiquitination enzyme	Normal	CG clusters	CG clusters
apc-2	Cell cycle	Ubiquitin ligase	Normal	CG clusters	CG clusters
sep-1	Cell cycle	Chromosome segregation	Normal	Normal	Retained CGs
ify-1	Cell cycle	Separase regulation	Normal	Normal	Retained CGs
cdk-1	Cell cycle	Entry into M phase	Normal	Normal	Retained CGs
cks-1	Cell cycle	Cell cycle exit/cytokinesis	Normal	Normal	Absent
chs-1	Cargo	Chitin synthesis	Normal	Normal	Absent
sqv-4	Cargo	Glycosylation enzyme	Small CGs	Small CGs	Absent
cpg-1/-2	Cargo	Chitin-binding proteins	Small CGS	Small CGs	Absent